

CrystEngComm

Accepted Manuscript



This is an *Accepted Manuscript*, which has been through the Royal Society of Chemistry peer review process and has been accepted for publication.

Accepted Manuscripts are published online shortly after acceptance, before technical editing, formatting and proof reading. Using this free service, authors can make their results available to the community, in citable form, before we publish the edited article. We will replace this *Accepted Manuscript* with the edited and formatted *Advance Article* as soon as it is available.

You can find more information about *Accepted Manuscripts* in the [Information for Authors](#).

Please note that technical editing may introduce minor changes to the text and/or graphics, which may alter content. The journal's standard [Terms & Conditions](#) and the [Ethical guidelines](#) still apply. In no event shall the Royal Society of Chemistry be held responsible for any errors or omissions in this *Accepted Manuscript* or any consequences arising from the use of any information it contains.

Direction of the Polymorphic Form of Entacapone using an Electrochemical Tuneable Surface Template

Ana Kwokal^a and Kevin J. Roberts^{b*}

Abstract

The ability to direct the surface crystallisation of different polymorphs of entacapone by tuning the electrochemical potential of Au(100) templates is demonstrated. Under quiescent conditions, without polarization (at open circuit potential), entacapone crystallises in its stable form A on the template surface and concomitantly in its metastable form D in the bulk solution. When Au(100) is negatively polarized (-150 mV), form D is still formed in the bulk solution but the metastable form α is found to crystallise at the edges of the template. Both crystals of form A and α were observed to grow epitaxially over the Au template surface. The electrochemical templating effect is consistent with the polarisation changing the structure of the initially adsorbed layers of supersaturated solution at the template surface which directs the nuclei formation and the subsequent crystal growth processes. This study demonstrates, for the first time, the direction of polymorphic form using a low field polarized nucleation template.

Introduction

Despite the rather extensive research carried out over the years, the ability to direct and manipulate the crystallization processes to produce a selected polymorphic system is still rather limited. This, in turn, can restrict the capability of researchers and industrial practitioners to control and optimise the processes needed for the development and manufacture of high quality pharmaceutical and fine chemical products. A critical step in polymorphic control lies in achieving effective control of nucleation stage as this represents the key formative stage of the molecular assembly process where the local intermolecular arrangement is defined.

From a phenomenological perspective, nucleation in crystallisation systems is mostly heterogeneous with the process being initiated at preferred local sites where the molecular-scale functionality of an available substrate provides a suitable structural environment for its promotion. In practical process systems, such substrates include vessel/piping walls¹⁻³, impellers, baffles, probes used for analytical instrumentation⁴ etc. Structural matching between the hetero nucleation substrate and the surface functionality of the crystallising product⁵⁻⁸ and/or the porosity/confinement provided by the micro/nano scale geometry and porosity of the substrate⁹⁻¹¹ are important factors in this respect.

However, electrochemical interactions within the interfacial double-layer at the nucleation interface that mediates substrate-product attachment process together with the structure of the initially adsorbed layers can be expected to play a significant role in mediating surface-induced nucleation. For example, the fact that L-glutamic acid exhibits differences in its nucleation behaviour when crystallised in a batch reactor with two different stirrer materials, electronegative and hydrophilic stainless steel and electropositive and hydrophobic polymers for an otherwise identical process, is particularly informative¹². Presumably, for solution phase crystallisation,

such surface polarisation effects impact on the ability of solute molecules to adsorb at the substrate/solution interface, particularly for polar solute and solvent species. Such effect can direct the nucleation process to more energetically favoured surface nucleation sites at the expense of a less favoured bulk nucleation process. Through this approach specific molecules can thus be preferentially adsorbed from bulk solution at a substrate surface provided that its electrochemical surface potential is sufficient to promote the molecular assembly of suitable nuclei. Mindful that different adsorbed species can have different polarisabilities, by tuning the surface potential, it should be feasible to modify the absorption selectivity of the various species with a concomitant impact upon the resulting structure of material formed. The direction of surface properties is, of course, of fundamental importance in electrochemistry where variation in surface potential has long been used to initiate crystallisation and phase conversion at electrode surfaces.¹³⁻¹⁶

Previous studies have also shown that the crystalline solid form (polymorph, morphology etc.) could be changed by modifying the surface and interfacial properties using single crystals of metals such as gold¹⁷, organic crystals^{8, 18, 19}, polymers²⁰⁻²², Langmuir monolayers^{23, 24} and, in particular, by the nucleation templates provided by surface assembled monolayers (SAMs)²⁵⁻²⁷.

Electrochemical techniques are another powerful method for building nanostructures on solid surfaces. Using these techniques, one can easily obtain stable monolayers or sub-monolayers with well-ordered and tailored structures. Moreover, the arrangement of such structures can be changed through the application of very low applied electrochemical potentials. For example, the charge density at an electrode surface can be fine-tuned by an external electric field which can change the configuration and strength of surface adsorption and even result in the formation of different surface structures.²⁸⁻³⁷

To the authors' knowledge there has been no published research in which low magnitude *dc* polarisation has been applied to a SAM template with the aim to effect the direction and control of the polymorphic form. Previous studies have, though, demonstrated that strong electric fields can be used to enhanced crystal nucleation,^{38,39} promote the preferred orientation of crystals⁴⁰ and to direct polymorphs.⁴¹ Low strength *ac* fields⁴² have also been found to reduce a number of nucleation sites and enhance quality of crystals. Similarly, low *dc* electric fields have been used to control the spatial and temporal localisation of nucleation, decrease the number of surface nuclei and increase the size and quality of protein crystals.⁴³⁻⁴⁵

Recent research^{46,47} by this group have demonstrated that under quiescent conditions Au(100) and Au(111) surface template can direct the formation of form A at its surface with the concomitant crystallisation of form D in the bulk solution. In 100% of the cases form D crystallise spontaneously from that particular solution and supersaturation. In agitated solutions, hydrodynamic forces were found to detach the particles from the template surface effecting the seeding of the bulk solution and resulting in the formation of only form A throughout the vessel.

In this communication, the latter work was further developed though a consideration as to whether the application of an electrochemical-induced change in the surface polarisation of the gold (Au(100)) template might affect the nucleation phenomena previously characterised. Additionally, the similar behaviour observed for Au(111) was exploited to enable separation of the template/crystal interface through which

the crystal orientation and resultant surface chemistry associated with the interface was elucidated.

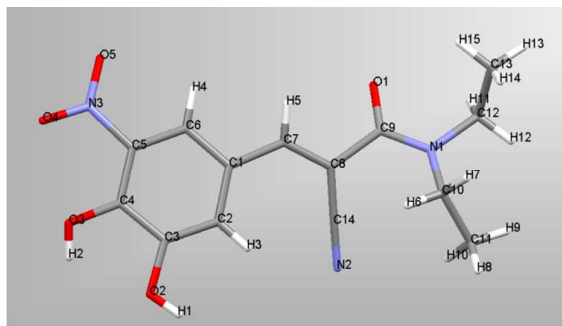


Figure 1 The molecular structure of entacapone (*E*)-2-cyano-*N,N*-diethyl-3-(3,4-dihydroxy-5-nitrophenyl) propenamid).

Experimental Details Entacapone, (*E*)-2-cyano-*N,N*-diethyl-3-(3,4-dihydroxy-5-nitrophenyl) propenamide was provided by courtesy of PLIVA Croatia Ltd. with about 99.9% purity and used for these studies. The mixed solvent system 88% (vol/vol) of the distilled water and 12% (vol/vol) of the acetone (Acros Organic p.a.) was used. Both Au(100) and Au(111) surfaces were prepared. The former was provided by Goodfellow Ltd. in the form of a single crystal cylindrical disc (0.5 cm diameter, 1 mm thick, $\pm 3^\circ$ in crystal orientation and < 99.99% of; purity). This sample was also used for the electrochemical studies. The latter was prepared through vacuum sputtering of a thin film of gold onto the cleaved basal plane of a mica substrate.

The Au(100) surface was cleaned through the following procedure: polishing with 1200 SiC paper, rinsing with the tap water, 5-minute sonication, immersion in a 3:1 mixture of concentrated sulphuric acid and 30% hydrogen peroxide for 15 minutes, and rinsing with the distilled water and then with the acetone. No cleaning procedure was needed for the Au(111) surfaces as these were freshly prepared and were kept sealed under a nitrogen atmosphere prior to use.

Crystallisation experiments were carried out at room temperature using the clean Au(100) and Au(111) surfaces which were immersed and secured in a vertical position within a 100 ml glass beaker containing a quiescent supersaturated entacapone solution. The solution was prepared by the dissolution of the solute in acetone followed by addition of water to the desired concentrations $c = 0.3$ g/L and supersaturation $\sigma = 2.0$, where the latter was defined as $\sigma = (c - c^*) / c^*$ and c^* is equilibrium concentration. At room temperature $c^* = 0.1$ g/L.⁴⁶ The vessel was covered and left undisturbed under the ambient conditions for about 12 hours.

The Au(100) template was also examined at negative electrochemical polarization. The latter was effected using a conventional three-electrode cell with Au(100) as a working electrode, a platinum sheet as counter electrode and Ag/AgCl as the reference electrode. Polarization was assured using an EG&G Princeton Applied Research potentiostat/galvanostat Model 283.

Entacapone crystals grown at the Au(100) and Au(111) interfaces were harvested and characterised by X-ray powder diffraction (Philips X'Pert with zero background holders). The crystals attached to the surface were analyzed *in-situ* using FTIR reflectance microscopy (Continuum μ M by Thermo Spectra Tech with a mirror gold plate used for a background), optical microscopy (Olympus BX51); scanning electron

microscopy (Philips XL30) and by single crystal methods (Oxford Diffraction Xcalibur diffractometer; Sapphire CCD detector; $2\theta = 3.4\text{--}61.4^\circ$; Cu K_α radiation; $\lambda = 1.54$; omega-scan data collection using CrysAlisPro, Oxford Diffraction Ltd).

Results and Discussion The electrochemical behaviour of gold in mixed aqueous/acetone solutions, as studied using cyclic voltammetry, both with and without the presence of entacapone in the solution, has been previously described.²⁸ In this study two different potentials were chosen to test the influence of template polarisation on crystallisation behaviour; the open circuit potential (at about 200 mV) in which entacapone spontaneously adsorbs and the negative potential of -150 mV where the surface is free from gold oxide and hydrogen evolution is not evident. The latter conditions are consistent with an electric field strength of ca. 8 Vm^{-1} .

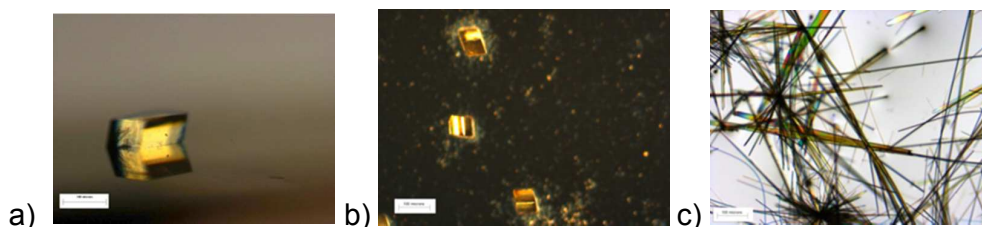


Figure 2 Optical micrographs of entacapone crystals as produced following quiescent solution crystallisation: (a) form A on Au(100); (b) form A on Au(111); (c) form D grown within the bulk solution.

Crystallisation of entacapone in the presence of both Au(100) or Au(111) templates under open circuit potential conditions revealed that prismatic crystals of form A formed at the surface (Figure 2(a),(b)) in contrast to form D (Figure 2(c)) that was found to concomitantly crystallise in the bulk solution at the bottom of the beaker. A more detailed SEM examination of the crystals nucleated on the Au(111) surface (Figure 3 (a)) revealed high quality crystals with a well-defined equant and ‘cube-like’ crystal morphology characterised by very smooth facet surfaces and nearly perfect facet edges consistent with epitaxial growth at the template/solution interface. The crystal orientation with respect to the nucleating interface was mostly through binding to the dominant “cube” surfaces of entacapone although a small number of crystals were found to adopt other orientations. These well-defined and non-random nature of the crystal orientation was consistent with a template-directed surface oriented growth process. The entacapone crystals formed on both the Au(100) or Au(111) surfaces were analysed *in-situ* and confirmed by IR microscopy and XRD to be of the stable form A.

The structural relationship between the crystal habit surfaces of the individual entacapone crystals and Au(111) interface was examined in further detail using XRD texture analysis. The X-ray pattern of Au(111) template with entacapone crystals grown at its surface (Figure 3(b)) reveals the crystallographic (010) face to be the preferential orientation with respect to the gold surface. This was confirmed through the analysis of an individual crystal using single crystal X-ray diffraction. The latter was analysed by peeling off the gold and one of the mica layers from the substrate together with its entrained entacapone crystals with the associated interfacial crystal plane being indexed by XRD. In this, the (010) crystal plane of form A was found to be attached to the surface revealing that this lattice plane of the entacapone crystal was bound to the Au(111) surface. The orientation of the few crystals on the template surface in Figure 3 (a) which were not found to be aligned on their cube plane was qualitatively appraised suggesting that these were attached to the

interface either through their (0-11) or (011) habit planes. However, the preferential XRD orientation studies highlighted in Figure 3(b) would suggest that these other orientations are comparatively rare. Direct characterisation of the orientation of entacapone crystals on the (100) surfaces was not feasible due to the small size of the crystals and the difficulties inherent in separating the Au(100) thin film from its glass substrate. Nonetheless, examination of the morphologies of the crystals on both the mica and glass substrates was found to be consistent with the same epitaxial relationship.

Figure 4 shows the visualisation of the intermolecular packing present within the crystallographic unit cell⁵⁶ for the surface nucleated form A highlighting the (010) plane which appears to be the preferred crystal orientation for binding to the gold template. The likely functional groups available on this surface for binding would be the amino group through the nitrogen lone pairs or the cyano group through the cyano π -electron orbitals. The latter would appear to be more likely given the well-known propensity for this group for binding to gold.⁴⁸ This supposition is also consistent with work of Gilman et al.⁴⁹ who applied density-functional methods to study the adsorption of isocyanides on the gold (111) surface in which the cyano group was found to serve as an "alligator clip" to connect a molecule to metallic electrodes. Gilman et al.⁴⁹ also suggested that adsorption at both the hollow or atomic sites was feasible a conclusion which would be consistent with entacapone binding to the gold through cyano group regardless of the surface orientation and chemistry of the Au substrate, i.e. its structural functionality as a template. The latter probably explains the apparent ability for both the Au (100) and (111) surfaces to facilitate template formation and subsequent crystal nucleation. Further work is though clearly needed to clarify the detailed structural arrangement present within the Au/first-adsorption-layer/crystal multilayer nucleating interface. In this respect the application of polarised NEXAFS spectroscopy has particular utility for the determination of the surface orientation of thin organic layers⁵⁰⁻⁵⁵.

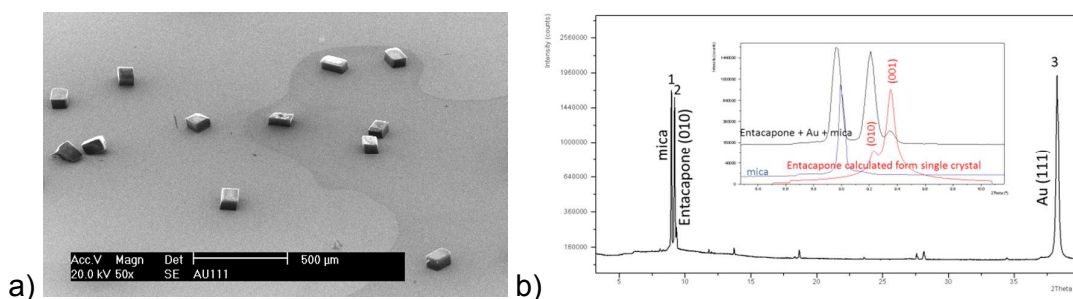


Figure 3 Structural characterisation of the crystal orientation of entacapone at the template interface: (a) SEM of form A crystals on Au(111); (b) XRD data showing diffraction peaks for (1) mica, (2) entacapone (010) and (3) Au (111). Inset (b): enlarged area (black) together with XRD data for mica (blue) and entacapone form A (red) as calculated from single crystal data.

The influence of a changing the polarisation of the gold/solution interface was carried out in order to see if the surface nucleation process could be "switched off" though electrochemical control under quiescent crystallisation conditions. Positive polarization was not employed since at these potentials the surface would be likely to be preferentially covered with gold oxide. A gold substrate was negatively polarized to -150 mV, i.e. to a potential just less than that needed for hydrogen evolution but within the range where the surface polarization charge would be significantly lower than the open circuit potential. A supersaturated entacapone solution was left to

crystallise in the presence of the negatively polarised interface overnight. Analysis of the results confirmed that crystals of form D were again crystallised at the bottom of beaker, i.e. within the bulk of solution. However, examination of the gold surface revealed it to be completely free of the array of nucleated form A crystals that had been previously observed under open circuit conditions. This observation thus confirms the system's ability to switch off the nucleation process at the template surface under electrochemical potential control. Mindful that under agitated conditions form D does not crystallise and that the surface nuclei of form A detach and grow in the bulk solution, then this ability to 'switch' the template effectively switches the whole batch crystallisation process. The latter, of course, is dependent on the supersaturation not exceeding the metastable limit for the bulk nucleation of form D.

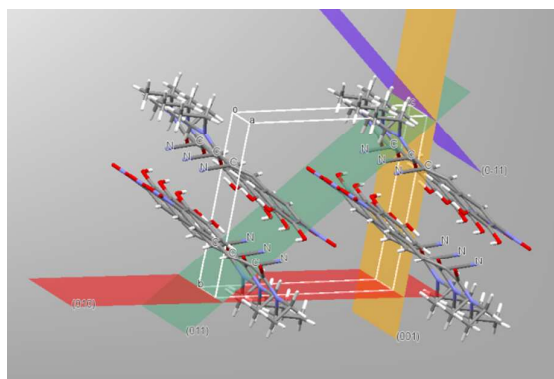


Figure 4. Inter-molecular packing within the crystallographic unit cell of form A entacapone based on the published crystal structure⁵⁶ highlighting and comparing the respective surface chemistry for the (010) – red ; (001) – yellow; (011) – green and (0-11) – violet crystal surfaces.

However, whilst crystals were not produced on the interface surface, a very small amount of crystals were formed at the edge of the interfacial electrode concomitantly with those of form D which were crystallised in the bulk solution. It was noteworthy, that these crystals were red in colour (Figure 5(a)) with an *in-situ* IR spectra that was not consistent with either forms A or D. XRD analysis of the detached red crystals identified these to be the metastable α -form⁵⁷ (Figure 5(c)). Repetition of this experiment confirmed the same observation. As these crystals were not grown as well-defined single isolated crystals, thus it was not feasible to determine their exact crystal orientation with respect to the substrate. Despite this, it is clearly evident that all the crystals formed had grown with a same orientation, most probably through epitaxial growth at the template edge.

This result suggests that the applied polarisation strongly influenced the adsorption tendency of entacapone to Au(100). The exact mechanism is not clear but this may relate to the ability of cyano or other functional groups of entacapone to potentially attach to a negatively polarised Au surface. Such a negative potential bias to the interface would be likely to favour adsorption of H^+ rather than cyano group. Alternatively, it may be that the negative polarisation simply does not promote the more ordered adsorption of entacapone seen under open circuit conditions which would potentially explain why crystals did not grow over the majority of the template surface. However, the observation of crystallisation at the electrode edges where the charge concentration and accessibility for solute mass transfer is much higher also suggests some selectivity to the templating process is afforded through heterogeneity of the adsorption site distribution. The fact that entacapone crystallised

as the metastable form α rather than the expected stable form A as previously observed under open circuit potential conditions implies that the firstly adsorbed layer structure has changed upon polarisation. This effect of polarisation-related structures of the first adsorption layer is well known and specially for cyanides.⁴⁸ Cyano group orientation over gold electrode is known to be dependant on surface polarity, i.e. when cyano group is attached through nitrogen lone pair electron the cyano group tends to be tilted significantly when electrode is negatively polarised. Moreover, it is known that CPAEt molecules that contain two cyano groups gives three different nanopatterns on Au(111) electrodes with respect to the applied potential region selected.³⁷ These authors have also shown that these patterns can be reversibly switched through the polarisation.

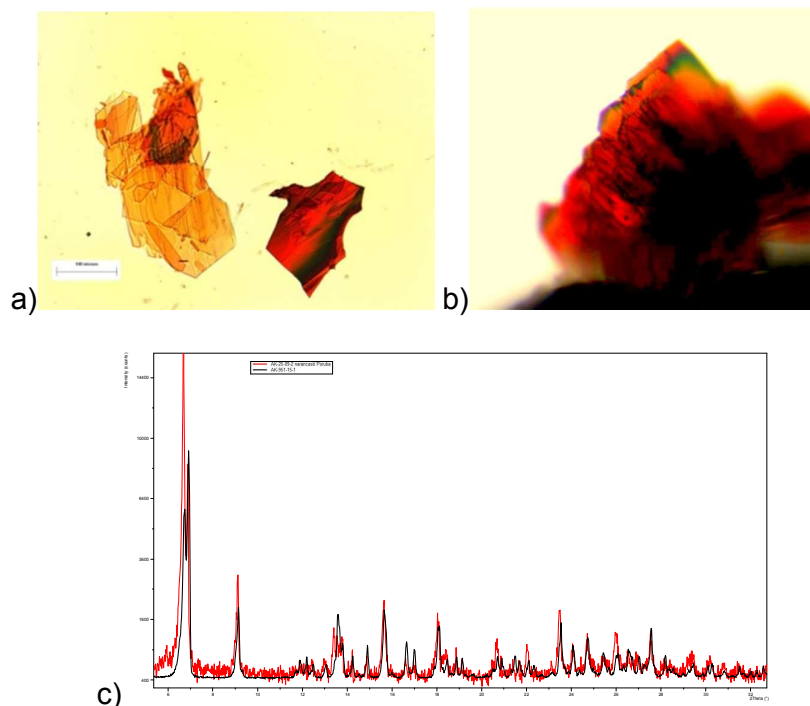


Figure 5. Characterisation of the entacapone α -form crystals produced on an Au(100) template polarised at -150mV vs. Ag/AgCl under potential control: (a,b) optical micrographs; (c) X-ray diffraction patterns (red) in comparison to reference data⁵⁷ (black).

These results are particularly interesting in that the meta-stable α -form of entacapone has only previously been prepared under non-equilibrium conditions by anti-solvent drop out or by interphase conversion from another polymorph form β .⁵⁷ This work, although preliminary in nature, suggests that electrochemical control might provide a useful additional process parameter for use in polymorphic screening and solid-form selection.

Conclusions

This study demonstrates the template-directed crystallisation of entacapone on Au(100) and Au(111) interfaces through behaviour consistent with the oriented adsorption of its solute molecules at the template/solution interface mediated through the preferential binding of the molecule's cyano functional groups to the template surface.

This study also provided clear evidence for the ability of electrochemical potential to control the surface nucleation process. Intriguing evidence was provided for the

ability for not just switch off the template under potential control but also regarding its use for directing the polymorphic form of the product crystals notably through the formation of the metastable α -form at negative potentials. The fact that the latter form crystallised on the template surface suggests that this interfacial system is highly selective with a supramolecular structure of the firstly adsorbed layers that mimics the appropriate intermolecular packing of the directed polymorphic form.

Although preliminary in nature, this work suggests the potential to apply the underpinning ideas of electrochemical-directed crystallisation more widely, particularly with a view to tailoring the molecular and supramolecular structure of the condensed interfacial template for wider applications to other systems. Previous work^{46,47} has also shown the utility of the generic approach underpinning the approach, particularly its potential for process scale up and through its utility as an alternative technology for the seeding of batch reactors.

For the pharmaceutical industry, the high quality of the materials produced through this technology confers an ability not only to engineer polymorphic selection but also to ensure high uniformity and low variability, in terms of the particle size and shape of the resultant product form. The latter resonates very strongly with growing demands of the regulatory agencies, such as the FDA, for a much greater emphasis on process understanding through application of quality by design approaches in the future development of process for the manufacture of new drug candidates.⁵⁸

Notes and references

^a *Pliva Croatia Ltd., Teva Pharmaceuticals, Research and Development, Prilaz baruna Filipovića 25, Zagreb, Croatia. ana.kwokal@pliva.hr*

^b *Institute of Particle Science and Engineering and Institute of Process Research and Development, School of Process, Environmental and Materials Engineering, University of Leeds, LS2 9JT, Leeds, UK, K.J.Roberts@leeds.ac.uk,*

* Communicating author

Acknowledgements

This work forms part of the doctoral studies⁵⁹ of one of us (AK) who gratefully acknowledges PLIVA Croatia Ltd. for their financial support during her study leave at the University of Leeds.

The authors are also most grateful to Dubravka Šišak from ETH Zurich, for her help with the morphological indexation of entacapone crystals and to Hugo Christenson and Chris Stephens in the Department of Physics at the University of Leeds for their help with the preparation of the Au (111) surfaces.

One of us (KJR) gratefully acknowledges the UK's EPSRC for their support in nucleation research at the Universities of Leeds and Manchester through their funding of the Critical Mass Project "Molecules, Clusters and Crystals" (grant references EP/I014446/1 and EP/I013563/1, respectively).

Reference

1. Y. Liu, Y. Zou, L. Zhao, W. Liu and L. Cheng, *Int. Commun. Heat Mass Transf.*, 2011, 38, 730-733.
2. F. Jones, P. Jones, R. De Marco, B. Pejčić and A.L. Rohl, *Appl. Surf. Sci.*, 2008, 254, 3459-3468.
3. H. Karoui, *Desalination*, 2013, 311, 234-240.

4. A. Borissova, S. Khan, T. Mahmud, K.J. Roberts, J. Andrews, P. Dallin, Z.P. Chen, E. Martin and J. Morris, *Cryst. Growth Des.*, 2009, 9, 692-706.
5. K. Chadwick, J. Chen, A.S. Myerson and B.L. Trout, *Cryst. Growth Des.*, 2011, 12, 1159-1166.
6. R. Hiremath, J.A. Basile, S.W. Varney and J.A. Swift, *J. Am. Chem. Soc.*, 2005, 127, 18321-18327.
7. A. Singh, I.S. Lee and A.S. Myerson, *Cryst. Growth Des.*, 2009, 9, 1182-1185.
8. M.D. Ward, *Chem. Rev.*, 2001, 101, 1697-1725.
9. B.D. Hamilton, I. Weissbuch, M. Lahav, M.A. Hillmyer and M.D. Ward, *J. Am. Chem. Soc.*, 2009, 131, 2588-2596.
10. Y. Diao, T. Harada, A. S. Myerson, T. A. Hatton and B. L. Trout, *Nat Mater*, 2011, 10, 867-871.
11. C.E. Nicholson, C. Chen, B. Mendis and S.J. Cooper, *Cryst. Growth Des.*, 2011, 11, 363-366.
12. K. Liang, G. White, D. Wilkinson, L.J. Ford, K.J. Roberts, W.M.L. Wood, K. Liang, G. White, D. Wilkinson, L.J. Ford, K.J. Roberts and W.M.L. Wood, *Cryst. Growth Des.*, 2004, 2, 1039-1044.
13. A. Balut, J. Robinson, K.J. Roberts, M.E. Herron and F.C. Walsh, *Jap. J. of App. Phys.*, 1993, 32, 422-424.
14. M.E. Herron, D. Pletcher, J. Robinson, S.E. Doyle, K.J. Roberts, R.J. Potter and F.C. Walsh, *J. Electroanal. Chem.*, 1995, 384, 39-46.
15. M.E. Herron, S.E. Doyle, K.J. Roberts, J. Robinson and F.C. Walsh, *Phase Transitions*, 1992, 39, 135-144.
16. S.E. Doyle, A.H. Nahle, K.J. Roberts, J. Robinson and F.C. Walsh, *T. Instit. of Met. Finish.*, 1994, 72, 63-65.
17. H. Teghidet, M.C. Bernard, S. Borensztajn, L. Chaal, S. Joiret and B. Saidani, *J. Cryst. Growth* 2011, 331, 72-77.
18. P.W. Carter and M.D. Ward, *J. Am. Chem. Soc.*, 1994, 116, 769-770.
19. S.J. Bonafede and M.D. Ward, *J. Am. Chem. Soc.*, 1995, 117, 7853-7861.
20. F. Lu, G. Zhou, H. Zhai, Y. Wang and H. Wang, *Cryst. Growth Des.*, 2007, 7, 2654-2657.
21. M. Lang, A.L. Grzesiak and A.J. Matzger, *J. Am. Chem. Soc.*, 2002, 124, 14834-14835.
22. S. Nauli, S. Farr, Y. Lee, H. Kim, S. Faham and J.U. Bowie, *Protein Sci.*, 2007, 16, 2542-2551.
23. I. Weissbuch, L. Leiserowitz and M. Lahav, *Curr. Opin. Colloid.*, 2008, 13, 12-22.
24. I. Weissbuch, R. Popvitz-Biro, L. Leiserowitz and M. Lahav, *The Lock and Key pinciple*, Wiley, New York, 1994.
25. A.Y. Lee, I.S. Lee, S.S. Dette, J. Boerner and A.S. Myerson, *J. Am. Chem. Soc.*, 2005, 127, 14982-14983.
26. I.S. Lee, A.Y. Lee and A.S. Myerson, *Pharm. Res.*, 2008, 25, 960-968.
27. A.Y. Lee, A. Ulman and A.S. Myerson, *Langmuir* 2002, 18, 5886-5589.
28. Z. Li, B. Han, L.J. Wan and Th. Wandlowski, *Langmuir*, 2005, 21, 6915-6928.
29. Z. Li, B. Han, L.J. Wan and T. Wandlowski, *Langmuir*, 2005, 21, 6014-6928.
30. G.J. Su, H.M. Zhang, L.J. Wan and C.L. Bai, *Surf. Sci.*, 2003, 531, L363-L368.
31. G.J. Su, H.M. Zhang, L.J. Wan, C.L. Bai and T. Wandlowski, *J. Phys. Chem. B*, 2004, 108, 1931-1937.
32. L.J. Wan, H. Noda, C. Wang, C.L. Bai and M. Osawa, *Chem. Phys. Chem.*, 2001, 10, 617-619.
33. J. Zhang, A.M. Kuznetsov, I.G. Medvedev, Q. Chi, T. Albrecht, P.S. Jensen and J. Ulstrup, *Chem. Rev.*, 2008, 108, 2737-2791.
34. F. Cunha, N.J. Tao, X.W. Wang, Q. Jin, B. Duong and J. D'Agnese, *Langmuir*, 1996, 12, 6410-6418.
35. Y. Dai, C. Meier, U. Ziener, K. Landfester, C. Täubert, and D. M. K. Langmuir, 2007, 23, 11058-11062.

36. Y. Diao, M. Han, L. Wan, K. Itaya, T. Uchida, H. Miyake, A. Yamakata and M. Osawa, *Langmuir*, 2006, 22, 3640–3646.
37. G. Su, Z. Li and R. Aguilar-Sanchez, *Anal. Chem.*, 2009, 81, 8741–8748.
38. M. Taleba, C. Didierjeana, C. Jelscha, J.P. Mangeota, B. Capelleb, A. Aubrya, J. *Cryst. Growth*, 1999, 200, 575–582.
39. A. Penkova, O. Gliko, I.L. Dimitrov, F.V. Hodjaoglu, C. Nanev, P.G. Vekilov, *J. Cryst. Growth* 2005, e1527-e1532.
40. C.N. Nanev, A. Penkova, *J. Cryst. Growth*, 2001, 232, 285-293.
41. J.E. Aber, S. Arnold, M.D. Ward, and B.A. Garetz, A.S. Myerson, *Phys. Rev. Letters* 2005, 94, 145503.
42. D. Hou and H. Chang, *Appl. Phys. Letters*, 2008, 92, 223902.
43. A. Moreno, G. Sazaki, *J. Cryst. Growth* 2004, 264, 438-444.
44. Z. Hammadi, J. Astier, R. Morin, and S. Veessler, *Cryst. Growth Des.*, 2007, 7, 1472-1475.
45. Z. Hammadi, J. Astier, R. Morin, and S. Veessler, *Cryst. Growth Des.*, 2009, 9, 3346-3347.
46. A. Kwokal, T. Nguyen and K.J. Roberts, *Cryst. Growth Des.*, 2009, 4, 4324-4334.
47. A. Kwokal, D. Čavuzić and K.J. Roberts, *Cryst. Growth Des.*, 2013, 13, 5324-5334.
48. J. Lipkowski and P.N. Ross, in *Molecular adsorption at Gold and Silver Electrodes*, eds. J. Lipkowski and L. Stolberg, VCH Publishers. Inc., New York, 1992, p. 171.
49. Y. Gilman, P.B. Allen and M.S. Hybertsen, *Phys. Rev. B.*, 2006, 112, 3314-3320.
50. G.P. Hastie and K.J. Roberts, *Langmuir*, 1995, 11, 4170-4172.
51. G.P. Hastie, J. Johnstone, K.J. Roberts and D. Fischer, *J. Chem. Soc.: Faraday Trans.*, 1996, 92, 783-791.
52. J. Johnstone, C.A. Peacock, K.J. Roberts, R.A. Hann, R.J. Oldman and S.K. Gupta, *Mol. Cryst. Liq. Cryst.*, 1996, 278, 157-164.
53. G.P. Hastie, J. Johnstone and K.J. Roberts, *J. Material Sci. Lett.*, 1998, 17, 1223-122.
54. J. Johnstone and K.J. Roberts, *Mol. Cryst. Liq. Cryst.*, 1996, 278, 27-36.
55. E. Ferrari, K.J. Roberts, D. Adams and M. Sansome, *Wear*, 1999, 236, 259-275.
56. J. Leppanen, E. Wegelius, T. Nevalainen, T. Jarvinen, J. Gynther and J. Huuskonen, *J. Mol. Struct.*, 2001, 562, 129-135.
57. D. Šamec-Škalec, M. Marinković, Z. Šiljkovic and M. Horvat., 2007, patent application number WO2007/135406.
58. Implementation of Quality by Design (QbD) - Current Perspectives on Opportunities and Challenges Topic Introduction and ICH Update, <http://www.fda.gov/downloads/AdvisoryCommittees/CommitteesMeetingMaterials/Drugs/AdvisoryCommitteeForPharmaceuticalScienceandClinicalPharmacology/UCM266751.pdf>.
59. A. Kwokal, *Tailor-made Batch Crystallization of Entacapone through the Use of Self-assembled Layers on Gold Surface* PhD, Thesis, *University of Zagreb, Croatia*, 2011.

